Available online at www.sciencedirect.com

jmr&t Journal of Materials Research and Technology

journal homepage: www.elsevier.com/locate/jmrt

Original Article

Changing the conventional clarification method in metal sulfide precipitation by a membrane-based filtration process

Humberto Estay [a,*], *René Ruby-Figueroa* [b], *Minghai Gim-Krumm* [a], *Gabriel Seriche* [a], *Michelle Quilaqueo* [a], *Simón Díaz-Quezada* [a], *Ignacio Cortés* [a,c], *Lorena Barros* [a]

[a] *Advanced Mining Technology Center (AMTC), University of Chile, Av. Tupper 2007 (AMTC Building), Santiago, Chile*

[b] *Programa Institutional de Fomento a La Investigación, Desarrollo e Innovación (PIDi), Universidad Tecnológica Metropolitana, Santiago, Chile*

[c] *Department of Chemistry, Universidad Tecnológica Metropolitana, Las Palmeras 3360, Ñuñoa, Santiago, Chile*

ARTICLE INFO

Article history:
Received 26 October 2020
Accepted 10 January 2021
Available online 20 January 2021

Keywords:
Metal sulfide precipitation
Membrane filtration
Microfiltration
Copper and cyanide recovery
SART process

ABSTRACT

The metal sulfide precipitation process is a widely studied technology used to recover metals or remove pollutants from different aqueous sources. However, the conventional clarification stage used to separate the generated precipitates cannot effectively remove them from recovered solutions. Taking this into account, the current study focuses on developing a new separation method applied in metal sulfide precipitates, based on a membrane filtration process. Different operating conditions and metal concentration in the feed solution were evaluated for the separation of copper sulfide precipitates formed from synthetic cyanide solutions in ceramic microfiltration membranes. Results showed attractive values of flux and copper recovery. Flux results ranged between 0.9 L/m^{2}s and 1.2 L/m^{2}s for copper concentrations above 500 mg/L, and copper recoveries resulted closer to 100% at the determined optimal operating conditions (4.5 pH, 120% NaHS stoichiometric dosage, and 2 bar feed pressure). These flux values decreased up to one order of magnitude for diluted copper concentrations, due to a change of aggregation capacity of precipitates. This study has demonstrated that the membrane filtration process can be a suitable alternative for the conventional gravitational clarification, promoting better performance results in terms of equipment capacity, metal recovery, and process safety.

* Corresponding author.
E-mail address: humberto.estay@amtc.cl (H. Estay).

https://doi.org/10.1016/j.jmrt.2021.01.034

1. Introduction

1.1. Metal sulfide precipitation

Both academia and industry have shown interest in the metal sulfide precipitation method, due to its ability to selectively separate dissolved metals from aqueous solutions, and simultaneously generate a product with a high concentration of the element recovered [1]. These features have been used to study the recovery of critical metals such as copper, cobalt, nickel, molybdenum, rhenium, zinc, palladium, and iron from different wastewaters and plant solution sources [2–18] or pollutants removal from different wastewaters, such as arsenic, antimony, and heavy metals [19–30]. The metal sulfide precipitation uses different types of sulfide sources (H_2S, NaHS, Na_2S, CaS, among others) to promote precipitation, as shown in the following general equation [1].

$$M^{2+} + HS^- \rightleftarrows MS_{(s)} + H^+$$

$$M^{2+} + S^{2-} \rightleftarrows MS_{(s)} \quad (1)$$

The low solubility of different metal sulfides facilities the separation process with high selectivity compared to other precipitates such as hydroxides or phosphates. Table 1 shows the solubility products of selected metals in the form of sulfide, hydroxide, or phosphate [31]. According to this data, metal sulfide species are highly insoluble, particularly in the case of silver, bismuth, copper, and mercury. In all cases, metal sulfide compounds are less soluble than metal hydroxides species. This is, in fact, the main advantage for environmental applications, particularly in terms of chemical stability, limiting its leaching or re-dissolution in waste deposits. In addition, the relative weight of the metal in the sulfide species is higher than hydroxides, because the molecular weight and oxidation number allow to reduce the mass of precipitates generated, reducing the costs of handling, transport, and disposal.

One of the main relevant applications is the selective removal of heavy metals from acid mine drainage (AMD) [6,22,26]. There is a considerable amount of research focused on the removal of metals from different wastewaters, such as acidic effluents from non-ferrous smelting processes [21,24,27,28] or electroplating industry [29,32]. Moreover, metal sulfide precipitation has been recently applied to recover critical metals from leach solutions generated in the treatment of different types of wastes. In particular, there is recovery of Co and Mo from wastes produced in the manufacturing of catalysts [3], recovery of Co from battery leachates [4], Re from smelting effluents [5], Mo, Ni and Co from the leachate of a mineral sludge [8], Ni, Co and Cu from leach liquor of Li ion battery recycling [11], Zn from leach solution of the treatment of fluorescent powder cathode tube [16], Mo, Ni and Co from a spent refinery catalyst leach liquor [17], Ni, Zn and Cu from plating process industrial raw effluent [25], Zn and Fe from the bioleaching treatment of mine tailings [12], and Cu, Fe, Zn and Mn from leach solutions of mine tailings using a fractional precipitation method [14]. The metal sulfide precipitation method is thus attracting great interest as a promising alternative method to move forward into the implementation of the circular economy concept due to its capacity to recover critical metals from waste processing.

Metal sulfide precipitation has been studied for its application as the primary treatment of pregnant leach solutions (PLS) in hydrometallurgical processes. This is the case of the application for recovering metals from the copper leaching PLS [2], Pd and Fe from acid solutions [7], Cu from glycinate-cyanide solutions [9], Cu from glycinate solutions [10], Cu, Mo and Zn from chloride solutions [13], Fe, Ni and Cu from bioleaching solution [15], or Cu and Zn from cyanide solutions in gold mining [33,34].

Accordingly, the use of alternative sources of sulfide has also been investigated, using oil fly ash [35], sulfur dioxide and sulfur [36], monocyclic pyrrhotite [37], and thioacetamide [38,39]. Similarly, the use of residual H_2S generated from a biological sulfate-reduction treatment to recover metals has been widely studied, particularly for the application in the AMD remediation [40–53].

A successful example of the application of the metal sulfide precipitation method at industrial scale has been the effective removal – and recovery – of copper with the regeneration of cyanide in gold mining. This process is known as SART (Sulfidization, Acidification, Recycling and Thickening), which has been installed in several cyanidation plants worldwide [33,54–58]. This process aims to remove copper from cyanide solutions, generating a saleable product, and also recovering cyanide (critical reagent to dissolve gold), which can be recycled to the leaching plant. Cyanide soluble copper minerals available in gold ores can increase the cyanide consumption from 0.2 to 0.5 kg NaCN/ton to over 2.0 kg NaCN/ton, causing a gold project to become infeasible, due to the rise of operational costs [54,59]. In cyanide media, the copper stable species is Cu^+, thereby the reaction defined in equation (1), in terms of copper precipitation from copper–cyanide complex, can be rewritten as follows [54].

$$2Cu(CN)_3^{2-} + 6H^+ + S^{2-} \rightleftarrows Cu_2S_{(s)} + 6HCN_{(aq)} \quad (2)$$

The effectiveness of the SART process, which reaches copper and cyanide recoveries of over 85%, has made feasible gold mine projects with a high content of cyanide soluble copper minerals in the ore [33].

Table 1 – Solubility products (logKsp) at 25 °C of selected elements. Adapted from [31].

Element	Sulfide	Hydroxide	Phosphate
Ag^+	−49.2	−7.9	−16.0
Bi^{3+}	−98.8	−31.0	−23.0
Cd^{2+}	−28.9	−14.3	−32.6
Co^{2+}	−22.1	−14.5	−34.7
Cu^+	−47.7	–	–
Cu^{2+}	−35.9	−19.8	−36.9
Fe^{2+}	−18.8	−16.3	–
Hg^{2+}	−52.2	−25.4	–
Mn^{2+}	−13.3	−12.7	–
Ni^{2+}	−21.0	−15.3	−31.3
Pb^{2+}	−28.1	−19.9	−42.0
Sn^{2+}	−27.5	−26.3	–
Zn^{2+}	−24.5	−16.1	−32.0

1.2. Conventional clarification of metal sulfide precipitates

The suspension formed by the precipitation reaction described in Eq. (1) must be clarified by a solid–liquid separation process, in order to generate (i) a treated solution with low solids contents, and (ii) a concentrated slurry or cake as the final metal product for further processing or disposal. The quality of the treated solution and, therefore, the efficiency of the separation step, is crucial to minimize the metal losses as well as the environmental point of view because the effluent must satisfy regulations and population health. Conventional solid–liquid separation is performed by gravitational clarifiers (thickeners) or filters [54,60]. However, another alternative, using lamella clarifiers, has been proposed to overcome the complexity of metal sulfide precipitates [19]. The above has driven several studies which were focused on understanding these precipitates with different characteristics, in order to predict or improve the solid–liquid separation performance [61–69]. The findings of these different studies have demonstrated the high variability of the separation performance, depending on the solution chemistry [61], the supersaturation control [62], operational conditions [63], and the interaction of each metal sulfide with water [67,68]. On the one hand, these precipitates can be strongly affected by the solution characteristics, particularly in particles with colloidal behavior [61–63,67]. On the other hand, there are metal sulfides, such as copper sulfides, which present a high aggregation capacity, increasing the particle size in these systems, and thereby improving its settling results [65,67,70]. In particular, copper precipitates have shown bi-modal behavior in a non-invasive optical microscopy and image processing and analysis, despite their high aggregation capacity [70]. These findings indicate that fine and colloidal particles remain in the suspension, promoting poor quality of clarified solutions (high solids content) in the conventional solid–liquid separation processes.

In order to address the above drawbacks, some studies have tried to modify certain characteristics of the suspension process to improve the settling performance. For example, the inclusion of additional metal ions [64], the inclusion of precipitates seeds to support a better nucleation [71], the effect of external ions in particle size and settling characteristics, such as calcium or magnesium [69], and the use of UV light irradiation during the precipitation reaction [72] have been explored for different metals and systems.

At an industrial scale, the SART process is an interesting application of metal sulfide precipitation and solid–liquid separation. This technology uses conventional gravitational clarifiers to separate the suspension formed in the precipitation reactor, and it also includes a recirculation of a part of the underflow into the reactor in order to theoretically increase the particle size of precipitates [33]. In the SART process, the clarification step has been declared the main challenge to be overcome when widening its application [73]. Clarification performance is affected by the complex nature of the precipitates that determines low settling rates and consequently large equipment size [33]. Correct operation in the clarification performance plays a crucial role, because it is where the copper and cyanide recoveries could lose 2 or 3 points, up to 40% of recovery under uncontrolled conditions [74]. SART application experience at industrial scale has shown some other detrimental consequences using conventional clarifiers such as: i) high residence time, which promotes the oxidation and further dissolution of copper, consequently decreasing the overall copper recovery, ii) copper dissolution also reduces the cyanide recovery, due to the formation of copper-cyanide complexes or by the generation of thiocyanate (SCN^-), according to the following reactions [65,75,76].

$$Cu_2S_{(s)} + 1/4O_2 + 2HCN_{(aq)} \rightleftarrows CuS_{(s)} + Cu(CN)_2^- + H^+ + 1/2H_2O \quad (3)$$

$$Cu_2S_{(s)} + 1/2O_2 + 2H_2S_{(aq)} \rightleftarrows 2CuS_{(s)} + H_2O \quad (4)$$

$$CuS_{(s)} + 5HCN_{(aq)} + 1/4O_2 \rightleftarrows 2Cu(CN)_2^- + 2SCN^- + 4H^+ + 1/2H_2O \quad (5)$$

In addition, the high surface contact between the slurry contained in the clarifier and the air promotes HCN volatilization [77]. This fact does not only reduce the overall cyanide recovery of the process, but it also increases the pH, generating the additional re-dissolution of copper because the reaction of Eq. (2) is displaced to the reactants [75]. Hence, the complex behavior of metal sulfide precipitates can determine large solid–liquid separation equipment and thereby detrimental performance consequences related to its associated high residence time. The drawbacks observed in the clarification step of the SART process using conventional thickeners must be taken into account for future applications of metal sulfide precipitation in other fields.

In the light of the previous information, there are new perspectives for the development of new technologies able to tackle the drawbacks observed in the traditional clarification process of suspensions obtained in the metal sulfide precipitation reactions. The improvement of the clarification step is linked to future implementation of these methods, facilitating the recovery of critical metals and the removal of toxic pollutants from different types of wastes, which are directly connected with the new perspective of circular economy.

1.3. Clarification by membrane filtration

Clarification by membrane filtration is one of the most common unit operations in different fields, including the food industry.

Membrane separation processes such as microfiltration (MF) and ultrafiltration (UF) are a valid alternative to address the drawbacks of conventional clarification. Both pressure-driven membranes have a series of advantages, including an increase in the yield process, a low quantity of steps, and therefore, they reduce working time, avoiding the use of clarifying agents, easy cleaning and maintenance of equipment, and waste product reduction [78]. Besides, membrane processes are characterized by their high-efficiency, simple equipment, and low energy consumption [79]. On the other hand, MF can be used to separate particles with diameters of 0.1–10 μm from a solvent and operate at low transmembrane pressure in the range of 0.5–4 bar. On the other hand, UF

operates at a hydrostatic pressure of 2–10 bar and allows the separation of molecules higher than the molecular weight cut-off (MWCO) of 1–1000 kDa [80]. In any membrane filtration, the retention of some particles leads to an accumulation of them on the membrane surface or fouling, producing a drop of the permeate flux. This flow reduction over time leads to losses in productivity, higher operating costs (as a result of higher energy costs), and increased maintenance requirements [81,82].

It should be pointed out that until these days, membrane filtration processes have not been applied to treat suspensions formed by metal sulfide precipitation processes, despite their characteristics indicate attractive possibilities with respect to the conventional clarifications methods. In this regard, the current study presents for the first time the application of membrane filtration (MF and UF) as a clarification method for suspensions of copper precipitates formed by sulfide precipitation method in cyanide media. Thus, an alternative to the conventional SART process is proposed to overcome the current limitations of the clarification stage in terms of overall metal recovery and clarification area required. The study involves the assessment of the main operational variables of the process, such as pH and sulfide dosage, the effect of copper concentration in the feed cyanide model solution, and the impact of the cyanide/copper (CN/Cu) molar ratio in clarification results.

2. Materials and methods

2.1. Experimental set-up and procedures

A prototype at laboratory scale was assembled, including a sealed, stirred and jacketed glass reactor of 2L capacity, connected with a membrane filtration module, through a diaphragm pump (KNF, Model NF 1.300TT18RC), as shown in Fig. 1. The monotubular ceramic membranes used were made of TiO_2, with an active layer of TiO_2–ZrO_2, 10 mm outer diameter, 6 mm inner diameter, 0.005 m^2 contact surface area (TAMI industries, Nyon, France), and 250 mm length. The tested membrane pore diameters for MF were 0.14 μm (hydraulic permeabilities to water ranged between 5.72×10^{-9} and 6.52×10^{-9} m^3 m^{-2} $Pa^{-1}{\cdot}s^{-1}$) and 1.4 μm (hydraulic permeabilities to water ranged between 1.56×10^{-8} and 1.69×10^{-8} m^3 m^{-2} $Pa^{-1}{\cdot}s^{-1}$). Additionally, a monotubular ceramic ultrafiltration (UF) membrane with 150 kDa cut-off was used (hydraulic permeability to water was 1.94×10^{-9} m^3 m^{-2} $Pa^{-1}{\cdot}s^{-1}$) for a specific test described later (section 2.3). The system was completed with a thermoregulates bath with recirculation (Jeio Tech, model RWE-2025), manometers located at the feed and retentate flows, and pH meter (Hanna instruments) immersed inside the reactor. The permeate flow was collected in a sealed tank, connected to the atmosphere through a tubing of 1 cm diameter, and located over a balance, which is also connected to a pc.

The solutions used were synthetic preparations, mimicking real characterizations of cyanide solutions used in gold mining [33,56,83]. The copper concentration was assessed within a range of 200 to 1800 mg/L, in order to cover the typical values of this metal found in gold mining. Demineralized water (<5 μS/cm) and analytical grade reagents were used for NaCN, CuCN, H_2SO_4, HCl, HNO_3, NaOH and NaHS (Sigma Aldrich, Merck). In case of H_2SO_4, NaOH and NaHS, 1M solutions were made to perform each test.

The copper metal sulfide precipitation reaction was conducted in the stirred reactor at 200 rpm agitation, where pH was also controlled during the reaction. After this time, the suspension generated in the reactor was pumped into the membrane module, so that the transmembrane pressure was controlled by a syringe valve in the retentate flow. The feed flow was defined in 650 mL/min, determining a cross flow velocity of 0.38 m/s. All tests were operated at 15 °C, regulated with a circulated water from a thermo-regulated bath connected to the reactor jacket.

The system was operated under batch concentration configuration, where the retentate flow was permanently recirculated into the reactor. The operation was finalized when the suspension contained in the reactor reached the minimum level to determine a concentration factor of around 10. To avoid HCN volatilization, the permeate tank received the permeate flow using a 1M NaOH solution. Before feeding the membrane module, samples were taken from the reactor from the permeate tank, and from the concentrated suspension contained in the reactor at the end of the test. The sample taken from the reactor at the end of the reaction was filtered using a syringe filter (0.22 or 0.02 μm). The filtered solution was

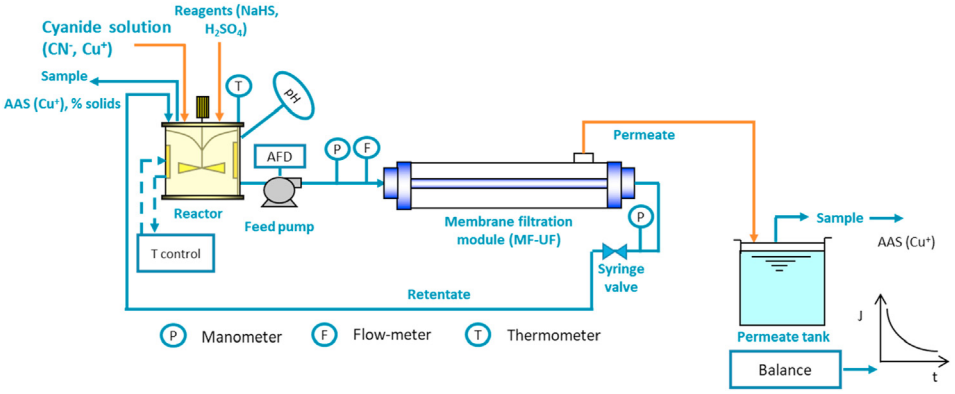

Fig. 1 – Laboratory prototype of metal sulfide precipitation coupled with membrane filtration process.

collected in a 1M NaOH solution. This sample and the permeate sample were analyzed for copper by atomic absorption spectroscopy (AAS, GBC model SensAA dual). The copper conversion was estimated through a mass balance, both at the end of the precipitation reaction (reactor copper conversion) and at the end of the membrane filtration test (overall copper conversion). In addition, the final sample taken from the concentrated suspension in the reactor was filtered, washed and then dried in a moisture balance to measure the solids content in the final slurry. Curves of flux with respect to the operating time were obtained from the permeate value measured by the balance. Thus, the flux value for each test was defined as the average between each point with a variation lower than 5%. Finally, membranes were washed by immersion for 24 h in a solution of HCl and HNO_3 both at 3% wt., recovering at least 85% of the original hydraulic permeability before it is used again.

2.2. Determination of critical transmembrane pressure and limiting flux

Limiting flux and critical transmembrane pressure (TMP) values were determined using a synthetic cyanide solution, which contained the highest copper concentration assessed in this study (1800 mg/L). The free cyanide concentration was set at 100 mg/L, simulating the typical conditions used in gold mining to dissolve gold [83]. The total cyanide concentration was determined using the same methodology described by Estay et al. (2020) [56]. This criterion defines a total cyanide concentration of 2460 mg/L. The copper sulfide precipitation step was conducted at 3.5 pH and 120% stoichiometric sulfide dosage in order to maximize the copper conversion and thereby the precipitates generated because a more severe fouling at these conditions was expected. The reaction time used was 15 min [33,56]. The suspension was then fed into the MF module, as described in section 2.1. The tests were performed varying the TMP in a range from 1 to 3 bar to obtain the limiting flux and the critical TMP [84,85].

This methodology was applied for MF membranes with 0.14 and 1.4 μm of pore diameter in order to define the adequate pore size membrane for the next tests. According to these results, the TMP and the pore size membrane were defined. The final copper conversion in the permeate was estimated to confirm maximum values and the membrane separation efficiency.

2.3. Effect of operating conditions and optimization

The effect of copper concentration, pH, and sulfide dosage in the membrane filtration performance was assessed, conducting an experimental program of Response Surface Methodology (RSM) based on a Box-Behnken design composed by 15 experimental runs, including three central points, and five degree of freedom for error [86]. All the computations were performed using Statgraphics Centurion XVI (Statgraphics Technologies, The Plains, VA, USA). Table 2 shows the factors and levels carried-out by the experimental program, and Table 3 shows the condition for each run. All tests were run at 2 bar of feed pressure, using a MF membrane of 0.14 μm of pore size, according to results obtained in previous tests (see section 3.1). The effects evaluated were flux and overall copper conversion. Based on the RSM results, the optimal conditions to maximize flux and copper conversion were estimated by the desirability function (DF) to determine the combination of variables to optimize multiple responses. The solids content in the remaining suspension contained at the end of each test in the reactor was measured. In addition, a qualitative analysis of aggregates shape and size to the concentrated slurry was conducted by optical microscopy (Leica DM 750 connected to a digital camera HD 5 MGPXL WI-FI, Leica ICC50W). A picture was taken for each test. A particle size distribution was determined particularly for run 10 of Table 3, using laser diffraction (Malvern Mastersizer 2000, Malvern Panalytical Ltd.,Malvern, UK).

Table 2 – Experimental design used to assess MF membrane performance.

Parameter	−1.0	0	+1.0
A: pH	3.5	4.25	5.0
B: Sulfide stoichiometric dosage, %	100	110	120
C: Copper concentration, mg/L	200	1000	1800

Additionally, an exploratory test of UF for run 10 was performed in order to assess the effect of a smaller membrane pore diameter for the lowest copper concentration evaluated in the study.

A final test was conducted with the aim of validating the optimal performance simulated by the desirability function (DF). This test was run at the determined optimal conditions (copper concentration, pH and sulfide dosage) determined previously. A sample of the final suspension remained in the reactor was taken, filtered, washed, and dried to a further X-ray fluorescence (XRF) analysis for determining the copper content in the precipitate.

The contribution of fouling resistance was determined using a resistance in-series model [87], as shown as follows:

$$J = \frac{\Delta P}{\mu\left(R_m + R_c + R_f\right)} \tag{6}$$

where J is the permeate flux (m^3/m^2s), ΔP is the pressure drop (Pa), μ is the liquid viscosity (Pa·s), R_m is the membrane

Table 3 – Detailed conditions for each run of the surface response analysis.

Run	pH	NaHS stoichiometric dosage, %	[Cu], mg/L
1	3.5	100	1000
2	5.0	100	1000
3	3.5	120	1000
4	5.0	120	1000
5	3.5	110	200
6	5.0	110	200
7	3.5	110	1800
8	5.0	110	1800
9	4.25	100	200
10	4.25	120	200
11	4.25	100	1800
12	4.25	120	1800
13	4.25	110	1000
14	4.25	110	1000
15	4.25	110	1000

Table 4 – Results of limiting flux and critical TMP for 0.14 and 1.4 μm pore size membranes ([Cu] = 1800 mg/L, CN/Cu = 3.34, pH 3.5, 120% stoich. NaHS).

Membrane pore size, μm	Limiting flux, L/m^2s	Limiting permeability, m^3/Pam^2s	Critical TMP, bar	Overall copper conversion, %
0.14	1.36	$4.5 \cdot 10^{-9}$	3.0	99.9
1.4	1.38	$9.2 \cdot 10^{-9}$	1.5	99.9

resistance related to the hydraulic conductivity (m^{-1}), R_c is the resistance related to the membrane fouling (m^{-1}), and R_f is the irreversible resistance related to membrane pore blocking and adsorption phenomena (m^{-1}).

2.4. *Effect of the residence time of sulfide precipitation stage*

Residence time effect on the permeate flux and copper conversion was evaluated in order to project their impact with a future perspective of scaling-up at pilot scale. In this regard, different residence time (5 and 10 min) was assessed over permeate flux and copper conversion.

2.5. *Effect of CN/Cu molar ratio on the clarification performance*

The tests conducted in previous sections (2.2–2.4) were carried out using a free cyanide concentration of 100 mg/L, which determined a CN/Cu molar ratio of 4.33, 3.44 and 3.34 for 200, 1000 and 1800 mg/L Cu, respectively. Taking into account that the total cyanide concentration value depends on the operating criteria of each cyanidation plant, and differences on the CN/Cu molar ratio could promote different results of permeate flux or copper recovery, tests focused on the effect of the CN/Cu molar ratio were also performed. In this regard, tests varying the CN/Cu molar ratio (3.34, 6.68, 10.0) for copper concentrations of 200, 500, 1000 and 1800 mg/L were conducted. This experimental program was run under univariate conditions that is each CN/Cu molar ratio was run for each copper concentration.

The sulfide precipitation stage was conducted at 5 min residence time, according to results obtained in the previous tests (see section 3.3), and the optimal conditions defined earlier for pH and sulfide addition (see section 3.2). Flux, copper conversion, and qualitative shape and size of aggregates taken from the optical microscopy were obtained for each test.

2.6. *Clarification performance for a highly concentrated cyanide solution*

Currently, the clarification stage of the SART process is also used to thicken as much as possible the slurry formed at the bottom of the equipment, in order to improve results in the further filtration stage. In this regard, the expected value used to design this process ranges between 10% and 15% [33], although there are no industrial results that confirm this criterion has been reached. Considering that the typical control used to thicken the underflow in conventional clarification processes is using the rise of the interface level of the slurry inside the equipment, the risk of increasing the solids content in the overflow increases. Therefore, it is highly probable that this dual requirement (high clarity of the overflow and high solids content in the underflow) in the clarification stage of the SART process promotes an opposite result, particularly in terms of the overflow clarity, reducing the overall copper and cyanide recovery in the plant. In this context, the possible achievement of a high quality permeate coupled by a retentate with high solids content by the MF process proposed here could be of high interest by the industry for future implementations.

The laboratory scale system described in section 2.1 is limited by the minimum level required by the pump. This limitation determines a maximum concentration factor of around 10, restricting the final solid concentration, considering the low copper concentration used in the feed solution. In addition, the volume of precipitate slurry obtained by each test would force it to blend the retentates in at least 10 tests. This possibility was dismissed by possible chemical changes with time, losing representativeness. Therefore, the assessment of the maximum solid content in the retentate must be performed using a high copper concentration in the feed solution. A high concentration of copper in the feed solution implies a high concentration of cyanide to avoid the precipitation of CuCN before the sulfide addition. For these reasons, a unique final test was performed at 21,000 mg/L Cu and 3.5 CN/Cu molar ratio, which is the minimum value to keep the copper dissolved, operating at the optimal conditions defined earlier (4.5 pH, 120% sulfide dosage, 2 bar feed pressure, 5 min residence time and 0.14 μm membrane pore size). The solid content was measured by a moisture balance from a sample taken from the final slurry contained in the reactor, to be finally filtered and washed.

3. Results and discussion

3.1. *Determination of critical TMP and limiting flux*

The limiting flux and critical TMP results are shown in Table 4. The limiting flux values are similar for both used membranes, although the critical TMP obtained for the 0.14 μm pore size membrane duplicated the value determined for the 1.4 μm. These results show that the fouling resistance formed by the copper sulfide precipitates determines a limiting flux near 1.4 L/m^2s. The differences between critical TMP values for both pore sizes can be explained by the intrinsic resistance of each membrane, which is higher for membranes with a lower pore diameter. When results are compared in terms of permeability, the 1.4 μm pore size membrane duplicated the value reached by the 0.14 μm pore size membrane.

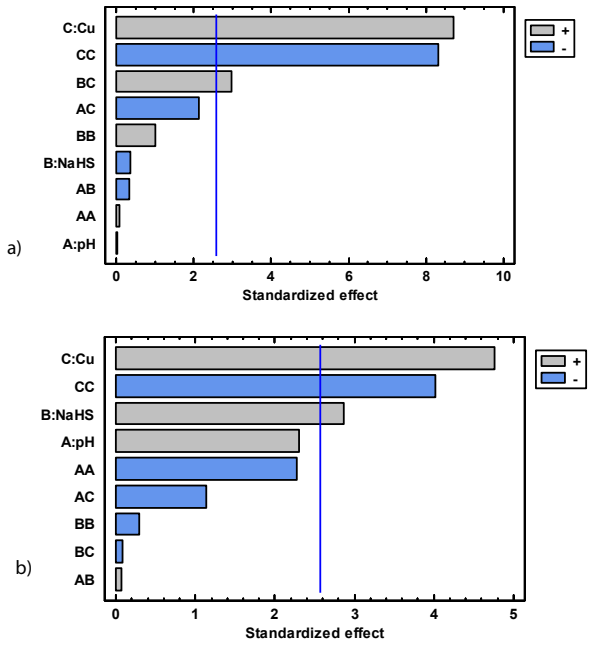

Fig. 2 – Standardized Pareto charts for flux (a) and overall copper conversion (b). Both charts show the interaction effect between each parameter (+) increases the effect response and (–) decreases the effect response.

The copper conversion reached values closer than 100%, confirming the aforementioned conditions defined where the operating conditions selected maximized the generation of precipitates. Moreover, these results indicate that both pore size membranes had a high rejection, because the content of dissolved copper in the permeate was neglected. In this respect, the safety measure taken, with regards to keeping a receiving NaOH solution in the permeate tank to avoid HCN volatilization, promotes the dissolution of copper precipitates, following equation (2). Therefore, any precipitate contained in the permeate solution must be detected by the analysis of dissolved copper.

Considering these results, where the maximum flux and rejection for both pore size are similar, but the critical TMP is lower for the higher pore size membrane, the selection of this last membrane could be attractive in order to reduce the energy requirements. Nevertheless, there are two additional aspects to be considered: i) Particle size distribution of these precipitates generated with the same conditions of those obtained for results in Table 3. Hence, they were measured by Mastersizer and a non-invasive optical microscopy method. In a previous report [70], they showed the possibility to have precipitates with sizes smaller than 1 μm, ii) The washing stage of the 1.4 μm pore size membrane took a long time with respect to the membrane of 0.14 μm pore size (data not shown). Therefore, there is a high possibility of pore clogging for the 1.4 μm membrane, promoted by the presence of smaller precipitates (<1.0 μm). Thus, the definition of feed pressure and membrane pore size was based on the minimization of this risk of severe fouling. Hence, the operating feed pressure was defined at 2 bar for the membrane of 0.14 μm pore size for the following assessments.

3.2. *Effect of operating conditions and optimization*

Fig. 2 shows the standardized Pareto charts for flux and overall copper conversion, where it can be observed the effect of each studied factor and the interaction effect between them. Factors or interactions overlapping the vertical blue line are considered statistically significant with a 95% confidence level. Thus, the most significant factor in both responses is the copper concentration in the feed solution. In the case of the overall copper conversion, the sulfide dosage has a minor effect on the response variable, but it is still significant. Taking these results into account, Fig. 3 shows the 3D response surface plot for flux and overall copper conversion as a function of the significant effects (copper concentration and sulfide dosage) at pH 4.25. According to these results, flux values ranged between 0.059 and 1.05 L/m^{2}s and overall copper conversion from 75% to 99.9%.

Flux results were surprisingly high when the values obtained here are compared with the hydraulic permeability of the membranes and by typical flux values reached by other matrices, which achieved up to two order of magnitude lower than those obtained here [85,88].

According to the hydraulic permeabilities reported in section 2.1, the maximum flux expected for water, in these membranes at 2 bar, ranges between 1.1 and 1.3 L/m^{2}s. Therefore, the maximum flux obtained in the clarification of copper sulfide precipitates is very close to the water flux, indicating low fouling impact. Nevertheless, the flux obtained drops almost by two orders of magnitude when copper concentration is as low as 200 mg/L.

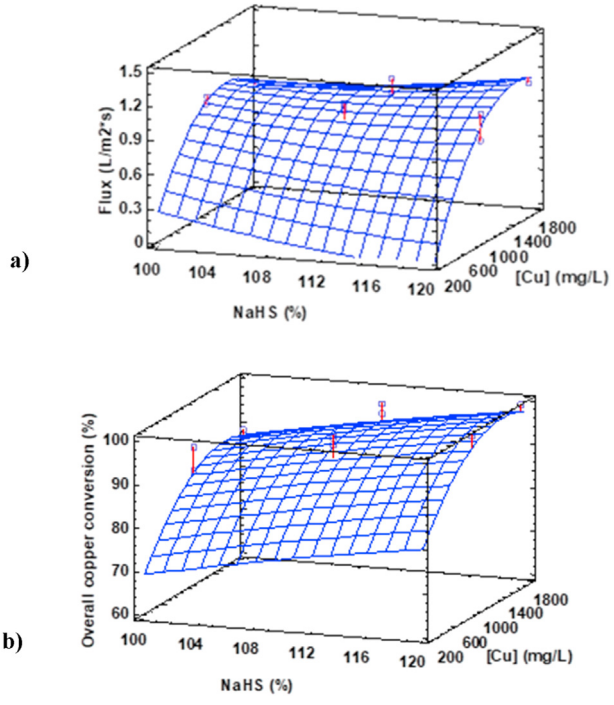

Fig. 3 – Surface response 3D curves for flux (a) and overall copper conversion (b) with respect to copper concentration and NaHS dosage at pH 4.25.

In addition, Fig. 4 shows selected curves from the experimental design for different copper concentration at the same sulfide dosage. These results show a highly stable flux curves for copper concentration over 1000 mg/L, defining values around 1.0 L/m^{2}s, instead of the flux at 200 mg/L Cu, where the curve is systematically decreasing up to achieve a plateau around 0.1 L/m^{2}s. Generally, it is reported that the increase in the feed concentration results in a drop in the permeate flux [89]; however, these work results are contrary to the expectations. The above can be explained by the differences in copper precipitates' shape and size characteristic at different copper concentrations.

The copper sulfide precipitates have previously been characterized at high copper concentration (1800 mg/L) [67,70], presenting high aggregation capacity and reaching aggregates sizes higher than 400 μm. Besides, the particle size distribution showed a bi-modal behavior with at least 30% particles under 10 μm. This aggregate size could explain the high flux values reached for higher copper concentrations, but it does not explain the flux drop at 200 mg/L Cu. In this case, the aggregation capacity of copper precipitates changes drastically, as can be seen in Fig. 5, where the size and shape of aggregates are compared for the same selected tests reported in Fig. 4. The aggregate size at 200 mg/L is slightly neglected in comparison to the aggregates formed at 1000 and 1800 mg/L Cu, which are larger than 200 μm. This size difference can explain the flux response for different Cu concentration because the associated type of fouling could be completely different.

Previous studies conducted by this research group [67,68], focused on the determination of the behavior of aggregation

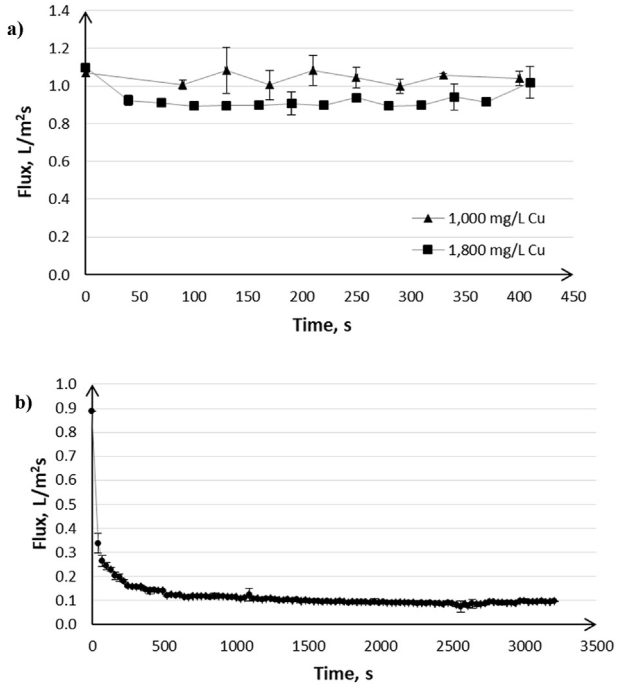

Fig. 4 – Flux vs time curves at different copper concentration in the cyanide feed solution at 110% sulfide stoichiometric dosage. a) [Cu] = 1800 (Run 8), and [Cu] = 1000 mg/L (Run 15), b) [Cu] = 200 mg/L (Run 5).

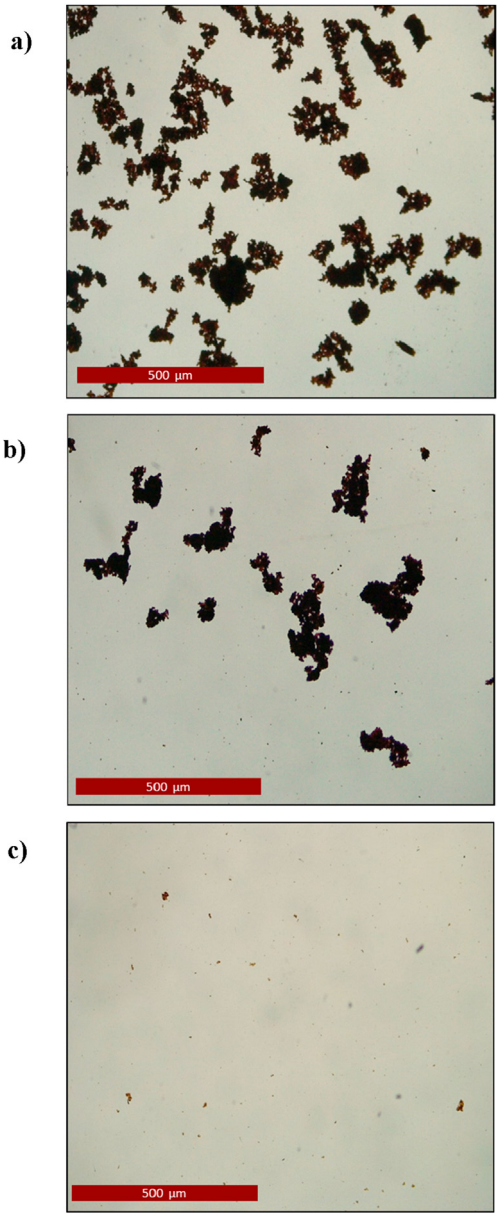

Fig. 5 – Optical micrographs of copper sulfide precipitates of selected tests at 110% sulfide stoichiometric dosage. a) 1800 mg/L Cu (Run 8), b) 1000 mg/L Cu (Run 15), c) 200 mg/L Cu (Run 5).

capacity of precipitates, suggesting that in case of copper precipitates, its interaction with water promotes the generation of large aggregates (electro static interaction between copper ions). Therefore, the high flux values reached at high Cu concentration can be promoted by the large aggregation size. Nevertheless, the aggregation capacity of copper precipitates at lower Cu concentration is negligible, as shown in Fig. 5. This behavior could be determined by the action of dissolved oxygen in precipitates, re-dissolving copper precipitates (Eqs (3) and (4)) and forming by-products such as SCN^- (Eq. (5)) or elemental sulfur, as shown in the following equation [65]:

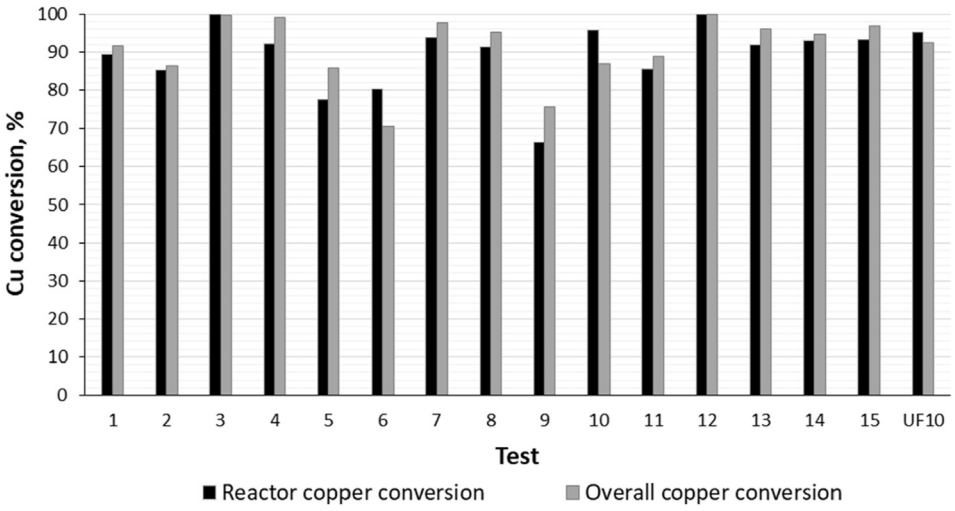

Fig. 6 – Copper conversion results obtained in the reactor (reactor copper conversion) and in the permeate (overall copper conversion) for each test of Table 3.

$$H_2S_{(aq)} + 1/2O_2 \rightleftarrows S^0_{(s)} + H_2O \quad (7)$$

The O_2/Cu molar ratio at lower copper concentration, maybe affects the growth of small aggregates by the action of thiocyanate (SCN^-), sulfur (S^0) or the oxygen itself on the surface of copper precipitates. This phenomenon limits the aggregation growth, promoting a different fouling formation on the membrane surface.

The overall and reactor copper conversions were compared to determine the separation efficiency of the membrane (Fig. 6). The overall copper conversion was higher than the reactor copper conversion in 13 out of 15 tests. This fact does not only confirms that the membrane filtration can keep at least the same copper conversion achieved in the reactor, but it also allows the copper conversion to be increased. In fact, the copper conversion for Cu concentration higher than 1000 mg/L was increased up to 7 points. The rise of copper conversion could be determined by the continuous HCN removal through the permeate along the membrane, which determines the shifts of the chemical equilibrium towards the products in the sulfide precipitation reaction (Eq. (2)). The occurrence of this phenomenon is a big difference to the current clarification performed by conventional gravitational thickeners, where the solution that contains the generated HCN remains together with copper precipitates. Instead, the membrane filtration process is continuously removing the products through the permeate flow.

In the case of tests carried out at 200 mg/L Cu (see Table 3), the copper conversion results are opposed. On the one hand, there are two tests where the overall copper conversion is higher than 8 points with respect to the reactor copper conversion (experimental runs 5 and 9). On the other hand, the only tests where copper conversion was high in the reactor occurred at 200 mg/L (experimental runs 6 and 10). Therefore, the low copper concentration condition does not only

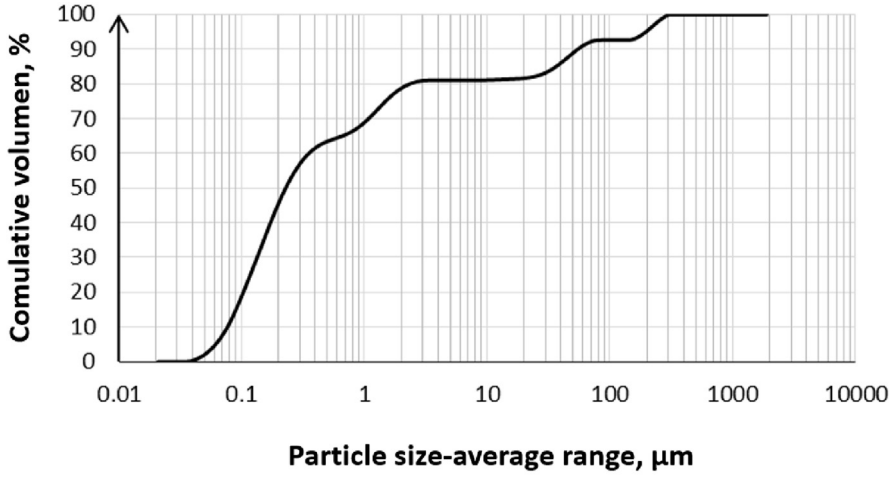

Fig. 7 – Cumulative particle size distribution of copper sulfide precipitates generated from a solution contained 200 mg/L Cu, at pH 4.25 and 120% sulfide stoichiometric dosage (Run 10), measured by Laser diffraction (Mastersizer).

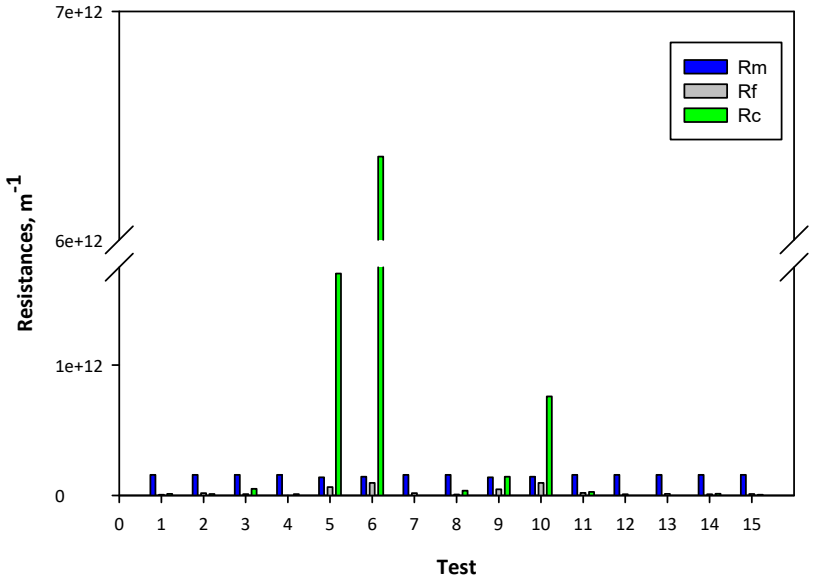

Fig. 8 – Distribution of resistances to permeation in tests of Table 3.

determines the lowest flux values, but it can also promote a decrease in the copper conversion. This fact can be explained by the dissolved oxygen effect, previously described, and the longer duration of these tests (Fig. 4), promoting copper dissolution (Eqs (3)–(5)), the presence of small precipitates that can cross the membrane, or a combined effect of both mechanisms. Fig. 7 shows the result of the cumulative particle size distribution of copper precipitates for run 10. This curve shows a 30% of particles smaller than 0.14 μm, defining a potential risk of pore clogging or particles crossing through the membrane. Therefore, the reason for the limited aggregation capacity of copper precipitates at low Cu concentration is a key aspect for the treatment of diluted feed flows. The possible detrimental effect of the dissolved oxygen for low copper concentration could be minimized at larger scale, under a steady-state condition, because the residence time of the process will be lower than the batch recirculation tests conducted here. Hence, the effect of dissolved oxygen on copper precipitates under cyanide media, and thereby its impact in the flux and also in the copper conversion must be carefully studied in future work.

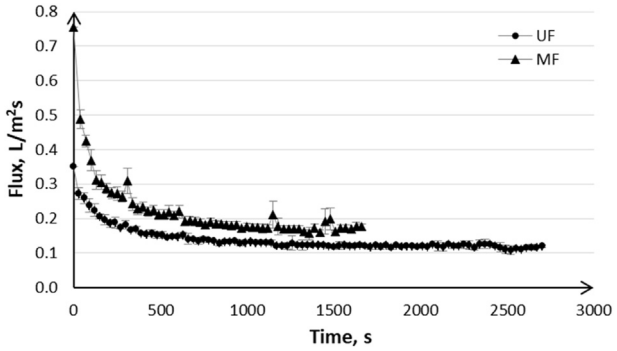

Fig. 9 – Flux vs time curves of MF and UF for Run 10 of Table 3.

The resistance in-series analysis (Fig. 8) related to Eq. (6) agrees with the previous results, showing that the membrane resistance (R_m) is more significant than the others resistances (R_c and R_f) for all tests of copper concentration higher than 1000 mg/L, with differences between one and two orders of magnitude. On the contrary, the R_c results for 200 mg/L copper concentration tests were significantly higher than R_m and R_f (al least one order of magnitude), even reaching above 90% resistance in tests 5 and 6 (Table 3). These results demonstrate a completely different behavior between the type of fouling and its effect on the permeate flux for low copper concentration. On the other hand, the values of irreversible resistance (R_f) for all tests were lower than 15% in agreement with the cleaning criteria of membranes. Future studies should focus on the determination of this value for longer times and after several washing steps. In this study, the recovery of membranes reached values of 100% after several washing steps without a concrete pattern of washing time, test condition, among others.

According to the aforementioned results obtained for Cu concentration of 200 mg/L, the future studies of metal sulfide precipitation coupled with membrane filtration must be conducted for the specific copper concentration expected in a

Table 5 – Optimal conditions simulated by the surface response method and the estimated responses to reach in these conditions.

Factor	Optimal value
pH	4.65
Stoichiometric NaHS dosage, %	119.98
Copper concentration, mg/L	1798.9
Response	**Result**
Flux, L/m^{2}s	1.12
Overall copper conversion, %	100.0

plant operation, including the determination of limiting flux and critical TMP.

In order to determine the effect of small particles and the long-time operation, an exploratory test of UF was performed at the same conditions of run 10. Fig. 9 shows the curves of flux vs time for MF and UF. Flux decreases from 0.18 to 0.2 L/m^{2}s in MF to 0.12–0.14 L/m^{2}s in UF (around 30% lower). Accordingly, the overall copper conversion increased from 87% in MF to 92.6% in UF, although is still lower than the copper conversion in the reactor (95.9 in MF, 95.4% in UF). This result indicates that particles lower than 0.14 μm could have crossed the MF membrane, but there is a fraction of copper precipitated in the reactor which is re-dissolved or still crosses the UF pores.

The solids content in the retentate varied from 0.37 to 0.67% wt., 1.0–2.0% wt., and 2.8–3.2% wt. for 200, 1000 and 1800 mg/L Cu, respectively, for all runs conducted.

According to the RSM a multiple optimization was performed (Table 5) to maximize the permeate flux and overall copper conversion. These results show that the flux and the overall copper conversion at high copper concentration could be maximum. The curve of flux vs. time obtained by the experimental validation test is shown in Fig. 10 (curve at 15 min), where pH slightly changed to 4.5. The curve shape is similar to those found for high copper concentration (Fig. 4a), and a stable flux value around 1.1 L/m^{2}s was reached. Likewise, the overall copper conversion was 99.9% (Table 6). These values validated the simulated results achieved by the multiple optimization. It is necessary to mention that the copper concentration in the feed solution cannot be adjusted, but the solids content in the precipitation reactor could be set by recycling part of the retentate flow. Thus, in this test, the optimal copper concentration of 1800 mg/L simulates a potential solids content in the reactor of around 0.2–0.3% wt. The effect of recycling and adjusting the solids content in the reactor must be confirmed by further specific tests, particularly to assess the effect of dissolved oxygen in the recycled precipitates.

Table 6 – Results of the effect of residence time in the precipitation reactor at the optimal conditions proposed (4.5 pH, 120% stoichiometric NaHS dosage, 1800 mg/L Cu).

Residence time, min	Solids content in retentate, %	Reactor copper conversion, %	Overall copper conversion, %
15	3.3	99.8	99.9
10	3.2	99.9	99.9
5	3.2	99.8	99.9

The results of elemental characterization by XRF analysis determined the following contents: 75.5% Cu and 20.3% S, confirming that the sulfide precipitation process can reach contents in solids closer to the stoichiometric value (in this case 79.9% Cu).

3.3. *Effect of residence time of sulfide precipitation stage*

The effect of residence time in the precipitation reactor is presented in curves of flux vs time in Fig. 10, and copper conversion and solids contents in retentate are shown in Table 6. Flux shows a slight decrease for residence times lower than 15 min, although the stable values are still kept around 1.0 L/m^{2}s. Moreover, the copper conversion was identical and maximum (99.9%) for the three times assessed. These results indicate that there is an opportunity of improving the reactor size without relevant effects on MF performance. In addition, these results are in agreement with the aggregate size evolution determined for 1800 mg/L copper concentration in a previous study [90], which showed that the maximum aggregation size was reached before 5 min of residence time.

3.4. *Effect of CN/Cu molar ratio on the clarification performance*

The cyanide content can modify the thermodynamic speciation of copper-cyanide complexes present in the feed solution, and thereby the stability of copper precipitates generated in

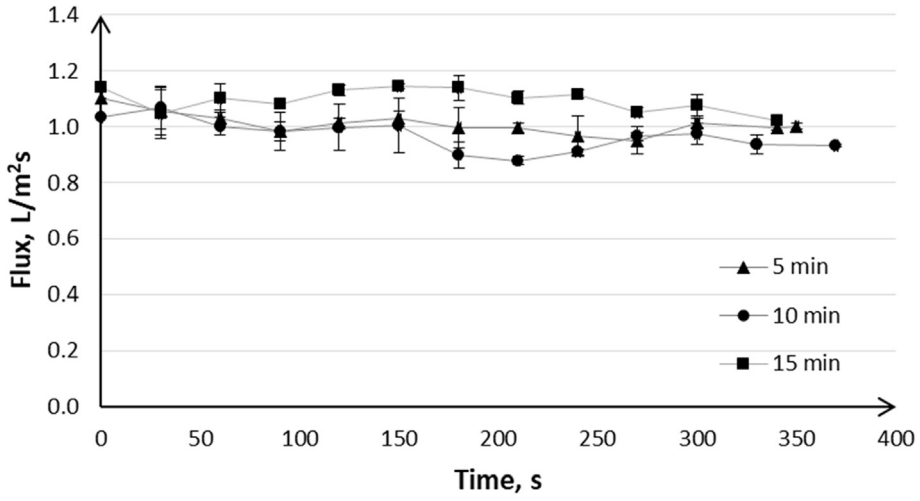

Fig. 10 – Flux vs time curves for different residence times in the precipitation reactor, obtained at the proposed optimal operating conditions (pH 4.5, 120% stoichiometric NaHS dosage, and 1800 mg/L Cu, 2 bar).

the sulfide precipitation stage, since the sulfide precipitation reaction could be displaced to reactants at higher CN/Cu molar ratio. Figure 11 shows the flux and copper conversion results for different CN/Cu molar ratio and copper concentration in the feed solution. These results show similar flux values for all CN/Cu molar ratio, when copper concentration is higher than 500 mg/L, keeping it in a range between 1.0 L/m^{2}s and 1.2 L/m^{2}s. In these conditions, it is particularly interesting that the flux results at 500 mg/L Cu are similar, and they even increases, to the one obtained for higher copper concentrations, indicating that the aggregation capacity in this condition is not affected as the one at 200 mg/L Cu (see Fig. 12a,b).

In the case of 200 mg/L Cu, the results show a drastic increase of flux at 10.0 CN/Cu molar ratio (over 250%) in comparison with the flux obtained at 3.34 CN/Cu molar ratio. This significant increase in flux is explained by the change of the aggregation capacity of copper precipitates at 200 mg/L Cu for 10.0 CN/Cu molar ratio (see Fig. 12c,d). Likewise, in this test, the overall copper conversion was higher than the reactor copper conversion by 2 points, demonstrating the relevance of the aggregate size on the process results. The only explanation to this phenomenon is coherent with the hypothesis of dissolved oxygen effects on the aggregation capacity at low Cu concentration. The detrimental effect of dissolved oxygen could be attenuated by the high presence of cyanide, which reacts with oxygen to form cyanate (CNO^-). The kinetic constant of this reaction should be sufficient slower than the kinetic of reactions from equations 3 to 5 and 7 in order to show a noteworthy effect only when the cyanide concentration is very high. Again, the understanding of the dissolved oxygen effect on the aggregation capacity of precipitates is a key aspect to optimize and maximize the performance of this proposed process for low copper contents.

3.5. *Clarification performance for a highly concentrated cyanide solution*

The final test to confirm the maximum tolerable solid content by the MF membranes show a stable flux curve over time, although there are slight drops related to the increase of solids concentration (Fig. 13), reaching flux values around 0.3 L/m^{2}s to 0.4 L/m^{2}s. The final solid content measured was 18.5% and the overall copper conversion confirms that the MF membrane could effectively reject the solids present in the treated suspension (Table 7). These results demonstrate that the membrane filtration is also capable of achieving a similar or

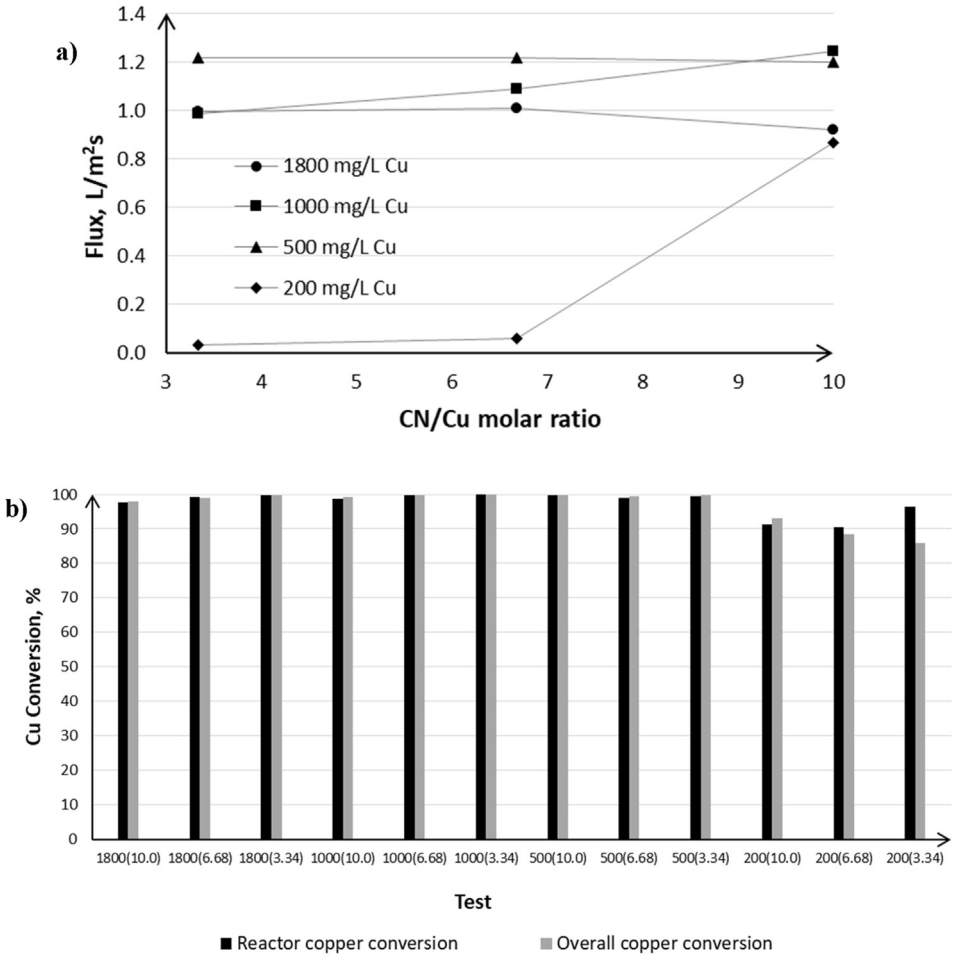

Fig. 11 – Results of the CN/Cu molar effect on flux (a) and overall copper recovery (b), obtained at the proposed optimal operating conditions (pH 4.5, 120% stoichiometric NaHS dosage, and 1800 mg/L Cu, 2 bar, 5 min). For graph (b) X-axis denotes Cu concentration (Cu/CN molar ratio).

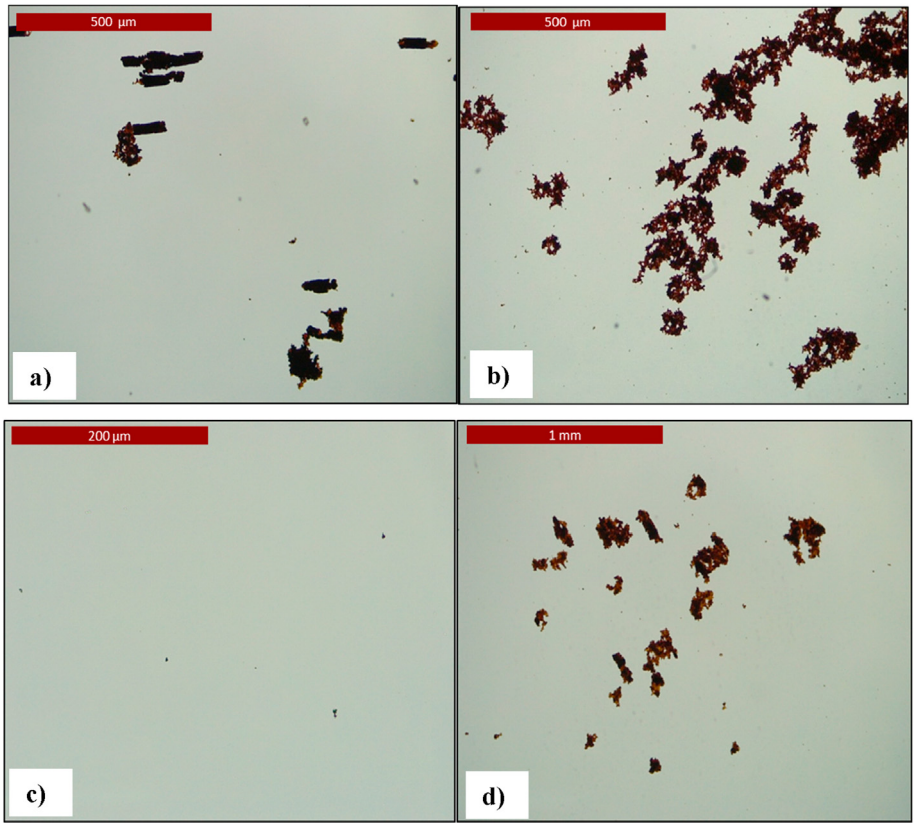

Fig. 12 – Optical micrographs of copper sulfide precipitates. a) 500 mg/L Cu at 3.34 CN/Cu, b) 500 mg/L Cu at 10.0 CN/Cu, c) 200 mg/L Cu at 3.34 CN/Cu, d) 200 mg/L Cu at 10.0 CN/Cu.

higher solids content in the final slurry in comparison with the SART process.

3.6. *Sizing approach*

According to the results obtained here, flux values for copper concentration over 500 mg/L were higher than 1.0 L/m^{2}s. In the treatment of an industrial flow of 200 m^3/h, the required membrane area will be 55.6 m^2 (without considering washing times). Industrial ceramic MF modules with this area have an approximate size of 1.2 m length and 0.5 m diameter (i.e., 0.24 m^3 equipment volume). The current clarification stage of a SART process uses thickeners designed with a rise rate of around 2.0 m^3/m^{2}h [33], showing a required area of 100 m^2, without safety factor, which defines a thickener diameter of 11.3 m: approximately 250 m^3 equipment volume. In terms of residence time, the membrane filtration process has a few seconds of residence time (<5 s) in comparison with a gravitational clarifier of the SART process, which is at least 90 min, depending on the cone angle. Furthermore, for lower copper concentration, where the membrane area could be 10 times higher, the total equipment volume and residence time will be several times lower than the conventional thickeners.

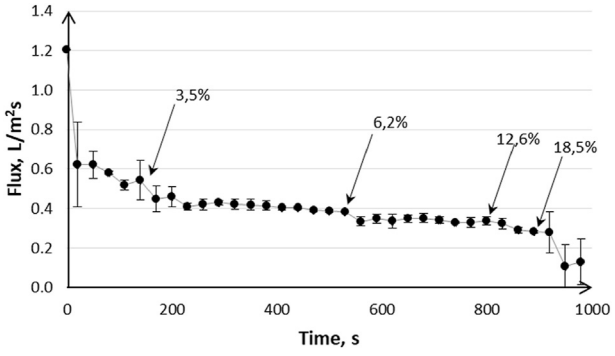

Fig. 13 – Flux vs time curve for a test of high copper concentration and optimal conditions (21,000 mg/L Cu, 4.5 pH, 120% stoichiometric NaHS dosage, 2 bar, 5 min).

The process based on membrane filtration proposed here can achieve better copper recoveries using less equipment volume, showing lower residence times with respect to the SART process. Thereby, this process avoids the risk or precipitates re-dissolution and cyanide losses given the detrimental effect of oxygen at high residence times. These advantages can reduce the capital and operational costs of a copper-cyanide recovery plant, by also increasing the income, and even reducing the contact area between suspensions and atmosphere, limiting the risk of HCN volatilization. Therefore, the proposed process here is more efficient and safer than the current clarification step of the SART process.

Finally, future studies must be focused on the validation of results with long time tests at steady-state, the understanding

Table 7 – Results of the final test at high copper concentration and optimal conditions (21,000 mg/L Cu, 4.5 pH, 120% stoichiometric NaHS dosage, 2 bar, 5 min).

Solids content in retentate, %	Reactor copper conversion, %	Overall copper conversion, %
18.5	89.4	91.5

of the effect of dissolved oxygen in the aggregation capacity of precipitates for low copper contents, membrane cleaning studies, and the impact of different impurities present in real cyanide solutions.

4. Conclusions

The current study was focused on developing a new process based on membrane filtration process for enhancing the clarification efficiency of copper sulfide precipitates in cyanide media. The work involved the study of the main effects of different operating conditions, the definition of feed pressure, reactor residence time, and maximum solid content produced in retentate and the impact of cyanide content in the process performance. The results were extremely promising, since flux values ranged between 0.9 L/m^{2}s and 1.2 L/m^{2}s for copper concentrations higher than 500 mg/L and copper recoveries closer to 100% at the determined optimal operating conditions (4.5 pH, 120% NaHS stoichiometric dosage, 2 bar feed pressure, and 5 min residence time). In addition, flux values dropped below 0.1 L/m^{2}s and overall copper recoveries were lower than reactor copper recoveries for copper concentrations of 200 mg/L, since the aggregation behavior of precipitates changed in this condition. The possible detrimental effect of dissolved oxygen must be studied in future works, in order to optimize these results. Regardless of these particular results at 200 mg/L Cu, which can be addressed using UF, the proposed technology shows attractive results with perspectives of an industrial implementation because it achieves better separation performance with respect to the conventional gravitational clarification, in terms of solids recovery, overall copper recovery, residence time, equipment capacity, and safety.

Declaration of Competing Interest

The authors declare that they have no known competing financial interests or personal relationships that could have appeared to influence the work reported in this paper.

Acknowledgments

The authors gratefully acknowledge the financial support of the National Commission for Scientific and Technological Research (CONICYT Chile) through the CONICYT-PIA Project AFB180004 and projects FONDEF/CONICYT 2017+ID17I10021 and FONDEF/CONICYT 2017+ID17I20021.

REFERENCES

[1] Lewis AE. Review of metal sulfide precipitation. Hydrometallurgy 2010;104:222–34. https://doi.org/10.1016/j.hydromet.2010.06.010.
[2] Hedrich S, Kermer R, Aubel T, Martin M, Schippers A, Barrie Johnson D, et al. Implementation of biological and chemical techniques to recover metals from copper-rich leach solutions. Hydrometallurgy 2018;179:274–81. https://doi.org/10.1016/j.hydromet.2018.06.012.
[3] Hamza MF, Roux JC, Guibal E. Metal valorization from the waste produced in the manufacturing of Co/Mo catalysts: leaching and selective precipitation. J Mater Cycles Waste Manag 2019;21:525–38. https://doi.org/10.1007/s10163-018-0811-9.
[4] Djoudi N, Le Page Mostefa M, Muhr H. Precipitation of cobalt salts for recovery in leachates. Chem Eng Technol 2019;42:1492–9. https://doi.org/10.1002/ceat.201800696.
[5] Hong T, Zheng T, Liu M, Mumford KA, Stevens GW. Investigation on the recovery of rhenium in the high arsenite wash acid solution from the copper smelting process using reducing sulfide precipitation method. Hydrometallurgy 2020;195:105402. https://doi.org/10.1016/j.hydromet.2020.105402.
[6] Zhang W, Honaker R. Process development for the recovery of rare earth elements and critical metals from an acid mine leachate. Miner Eng 2020;153:106382. https://doi.org/10.1016/j.mineng.2020.106382.
[7] Nanusha MY, Carlier JD, Carvalho GI, Costa MC, Paiva AP. Separation and recovery of Pd and Fe as nanosized metal sulphides by combining solvent extraction with biological strategies based on the use of sulphate-reducing bacteria. Sep Pur Technol 2019;212:747–56. https://doi.org/10.1016/j.seppur.2018.11.062.
[8] Vemic M, Bordas F, Comte S, Guibaud G, Lens PNL, van Hullebusch ED. Recovery of molybdenum, nickel and cobalt by precipitation from the acidic leachate of a mineral sludge. Environ Technol 2016;37:2231–42. https://doi.org/10.1080/09593330.2016.1146341.
[9] Deng Z, Oraby EA, Eksteen JJ. The sulfide precipitation behaviour of Cu and Au from their aqueous alkaline glycinate and cyanide complexes. Sep Purif Technol 2019;218:181–90. https://doi.org/10.1016/j.seppur.2019.02.056.
[10] Eksteen JJ, Oraby EA, Tanda BC. A conceptual process for copper extraction from chalcopyrite in alkaline glycinate solutions. Miner Eng 2017;108:53–66. https://doi.org/10.1016/j.mineng.2017.02.001.
[11] Calvert G, Kaksonen AH, Cheng KY, Van Yken J, Chang B, Boxall NJ. Recovery of metals from waste lithium ion battery leachates using biogenic hydrogen sulfide. Minerals 2019;9:563. https://doi.org/10.3390/min9090563.
[12] Ye M, Li G, Yan P, Ren J, Zheng L, Han D, et al. Removal of metals from lead-zinc mine tailings using bioleaching and followed by sulfide precipitation. Chemosphere 2017;185:1189–96. https://doi.org/10.1016/j.chemosphere.2017.07.124.
[13] Liu W, Sun B, Zhang D, Chen L, Yang T. Selective separation of similar metals in chloride solution by sulfide precipitation under controlled potential. JOM (J Occup Med) 2017;69:2358–63. https://doi.org/10.1007/s11837-017-2526-0.
[14] Chen T, Lei C, Yan B, Xiao X. Metal recovery from the copper sulfide tailing with leaching and fractional precipitation technology. Hydrometallurgy 2014;147–148:178–82. https://doi.org/10.1016/j.hydromet.2014.05.018.
[15] Cao J, Zhang G, Mao Z, Fang Z, Yang C. Precipitation of valuable metals from bioleaching solution by biogenic

sulfides. Miner Eng 2009;22:289–95. https://doi.org/10.1016/j.mineng.2008.08.006.
[16] Innocenzi V, De Michelis I, Ferella F, Beolchini F, Kopacek B, Vegliò F. Recovery of yttrium from fluorescent powder of cathode ray tube, CRT: Zn removal by sulphide precipitation. Waste Manag 2013;33:2364–71. https://doi.org/10.1016/j.wasman.2013.07.006.
[17] Cibati A, Cheng KY, Morris C, Ginige MP, Sahinkaya E, Pagnanelli F, et al. Selective precipitation of metals from synthetic spent refinery catalyst leach liquor with biogenic H_2S produced in a lactate-fed anaerobic baffled reactor. Hydrometallurgy 2013;139:154–61. https://doi.org/10.1016/j.hydromet.2013.01.022.
[18] Sampaio RMM, Timmers RA, Kocks N, André V, Duarte MT, van Hullebusch ED, et al. Zn–Ni sulfide selective precipitation: the role of supersaturation. Sep Pur Technol 2010;74:108–18. https://doi.org/10.1016/j.seppur.2010.05.013.
[19] Shammas NK, Wang LK. Sulfide precipitation for treatment of metal wastes. In: Wang LK, Sung Wang MH, Hung YT, Shamass NK, Chen JP, editors. Handbook of advanced industrial and hazardous waste management. Boca Ratn, FL: CRC Press, Taylor & Francis Group; 2018. p. 185–238.
[20] Hu B, Yang T, Liu W, Zhang D, Chen L. Removal of arsenic from acid wastewater via sulfide precipitation and its hydrothermal mineralization stabilization. Trans Nonferrous Met Soc China 2019;29:2411–21. https://doi.org/10.1016/S1003-6326(19)65147-2.
[21] Guo L, Du Y, Yi Q, Li D, Cao L, Du D. Efficient removal of arsenic from ''dirty acid'' wastewater by using a novel immersed multi-start distributor for sulphide feeding. Sep Pur Technol 2015;142:209–14. https://doi.org/10.1016/j.seppur.2014.12.029.
[22] Wang H, Chen F, Mu S, Zhang D, Pan X, Lee DJ, et al. Removal of antimony (Sb(V)) from Sb mine drainage: biological sulfate reduction and sulfide oxidation–precipitation. Bioresour Technol 2013;146:799–802. https://doi.org/10.1016/j.biortech.2013.08.002.
[23] Sun R, Li Y, Lin N, Ou C, Wang X, Zhang L, et al. Removal of heavy metals using a novel sulfidogenic AMD treatment system with sulfur reduction: configuration, performance, critical parameters and economic analysis. Environ Int 2020;136:105457. https://doi.org/10.1016/j.envint.2019.105457.
[24] Li H, Zhang H, Long J, Zhang P, Chen Y. Combined Fenton process and sulfide precipitation for removal of heavy metals from industrial wastewater: bench and pilot scale studies focusing on in-depth thallium removal. Front Environ Sci Eng 2019;13:49. https://doi.org/10.1007/s11783-019-1130-7.
[25] Zainuddin NA, Raja Mamat TA, Maarof HI, Puasa SW, Mohd Yatim SR. Removal of nickel, zinc and copper from plating process industrial raw effluent via hydroxide precipitation versus sulphide precipitation. IOP Conf Ser Mater Sci Eng 2019;551:012122. https://doi.org/10.1088/1757-899X/551/1/012122.
[26] Fu F, Wang Q. Removal of heavy metal ions from wastewaters: a review. J Environ Manag 2011;92:407–18. https://doi.org/10.1016/j.jenvman.2010.11.011.
[27] Zhang Y, Feng X, Jin B. An effective separation process of arsenic, lead, and zinc from high arsenic-containing copper smelting ashes by alkali leaching followed by sulfide precipitation. Waste Manage Res In Press. https://doi.org/10.1177/0734242X20927473.
[28] Zeng W, Guo W, Li B, Xiao R, Hu H, Yan Y, et al. Experimental and simulation studies of metal sulfide precipitates separation in copper smelting waste acid using a gravitation field-flow fractionation method. J Water Process Eng 2020;36:101330. https://doi.org/10.1016/j.jwpe.2020.101330.
[29] Islamoglu S, Yilmaz L, Ozbelge HO. Development of a precipitation based separation scheme for selective removal and recovery of heavy metals from cadmium rich electroplating industry effluents. Separ Sci Technol 2006;2041:3367–85. https://doi.org/10.1080/01496390600851665.
[30] Veeken AHM, Akoto L, Hulshoff Pol LW, Weijma J. Control of the sulfide (S^{2-}) concentration for optimal zinc removal by sulfide precipitation in a continuously stirred tank reactor. Water Res 2003;37:3709–17. https://doi.org/10.1016/S0043-1354(03)00262-8.
[31] Monhemius AJ. Precipitation diagrams for metal hydroxides, sulphides, arsenates and phosphates. Trans Inst Min Metall C 1977;86:202–6.
[32] Fang D, Zhang R, Deng W, Li J. Highly efficient removal of Cu(II), Zn(II), Ni(II) and Fe(II) from electroplating wastewater using sulphide from sulphidogenic bioreactor effluent. Environ Technol 2012;33:1709–15. https://doi.org/10.1080/09593330.2011.643319.
[33] Estay H. Designing the SART process – a review. Hydrometallurgy 2018;176:147–65. https://doi.org/10.1016/j.hydromet.2018.01.011.
[34] Estay H, Gim-Krumm M, Quilaqueo M. Two-stage SART process: a feasible alternative for gold cyanidation plants with high zinc and copper contents. Minerals 2018;8:392. https://doi.org/10.3390/min8090392.
[35] Rostamnezhad N, Kahforoushan D, Sahraei E, Ghanbarian S, Shabani M. A method for the removal of Cu(II) from aqueous solutions by sulfide precipitation employing heavy oil fly ash. Desalin Water Treat 2016;57(37):17593–602. https://doi.org/10.1080/19443994.2015.1087883.
[36] Hong T, Wei Y, Li L, Mumford KA, Stevens GW. An investigation into the precipitation of copper sulfide from acidic sulfate solutions. Hydrometallurgy 2020;192:105288. https://doi.org/10.1016/j.hydromet.2020.105288.
[37] Zhang X, Tian J, Hu Y, Han H, Luo X, Sun W, et al. Selective sulfide precipitate of copper ions from arsenic wastewater using monoclinic pyrrhotite. Sci Total Environ 2020;705:135816. https://doi.org/10.1016/j.scitotenv.2019.135816.
[38] Gharabaghi M, Irannajad M, Azadmehr AR. Selective sulphide precipitation of heavy metals from acidic polymetallic aqueous solution by thioacetamide. Ind Eng Chem Res 2012;51:954–63. https://doi.org/10.1021/ie201832x.
[39] Silva PMO, Raulino GSC, Vidal CB, do Nascimento RF. Selective precipitation of Cu^{2+}, Zn^{2+} and Ni^{2+} ions using $H_2S_{(g)}$ produced by hydrolysis of thioacetamide as the precipitating agent. Desalin Water Treat 2017;95:220–6. https://doi.org/10.5004/dwt.2017.21584.
[40] Xingyu L, Gang Z, Xiaoqiang W, Laichang Z, Jiankang W, Renman R, et al. A novel low pH sulfidogenic bioreactor using activated sludge as carbon source to treat acid mine drainage (AMD) and recovery metal sulfides: pilot scale study. Miner Eng 2013;48:51–5. https://doi.org/10.1016/j.mineng.2012.11.004.
[41] Papirio S, Villa-Gomez DK, Esposito G, Pirozzi F, Lens PNL. Acid mine drainage treatment in fluidized-bed bioreactors by sulfate-reducing bacteria: a critical review. Crit Rev Environ Sci Tech 2013;43:2545–80. https://doi.org/10.1080/10643389.2012.694328.
[42] Castro Neto ES, Aguiar ABS, Rodriguez RP, Sancinetti GP. Acid mine drainage treatment and metal removal based on a biological sulfate reducing process. Braz J Chem Eng 2018;35:543–52. https://doi.org/10.1590/0104-6632.20180352s20160615.
[43] Tabak HH, Scharp R, Burckle J, Kawahara FK, Govind R. Advances in biotreatment of acid mine drainage and biorecovery of metals: 1. Metal precipitation for recovery and recycle. Biodegradation 2003;14:423–36. https://doi.org/10.1023/A:1027332902740.

[44] Gopi Kiran M, Pakshirajan K, Das G. An overview of sulfidogenic biological reactors for the simultaneous treatment of sulfate and heavy metal rich wastewater. Chem Eng Sci 2017;158:606–20. https://doi.org/10.1016/j.ces.2016.11.002.
[45] Alam R, McPhedran K. Applications of biological sulfate reduction for remediation of arsenic - a review. Chemosphere 2019;222:932–44. https://doi.org/10.1016/j.chemosphere.2019.01.194.
[46] Altun M, Sahinkaya E, Durukan I, Bektas S, Komnitsas K. Arsenic removal in a sulfidogenic fixed-bed column bioreactor. J Hazard Mater 2014;269:31–7. https://doi.org/10.1016/j.jhazmat.2013.11.047.
[47] Janyasuthiwong S, Rene ER, Esposito G, Lens PNL. Effect of pH on Cu, Ni and Zn removal by biogenic sulfide precipitation in an inversed fluidized bed bioreactor. Hydrometallurgy 2015;158:94–100. https://doi.org/10.1016/j.hydromet.2015.10.009.
[48] Diez-Ercilla M, Sánchez-España J, Yusta I, Wendt-Potthoff K, Koschorreck M. Formation of biogenic sulphides in the water column of an acidic pit lake: biogeochemical controls and effects on trace metal dynamics. Biogeochemistry 2014;121:519–36. https://doi.org/10.1007/s10533-014-0020-0.
[49] Gallegos-Garcia M, Celis LB, Rangel-Méndez R, Razo-Flores E. Precipitation and recovery of metal sulfides from metal containing acidic wastewater in a sulfidogenic down-flow fluidized bed reactor. Biotechnol Bioeng 2009;102:91–9. https://doi.org/10.1002/bit.22049.
[50] Bilgin A, Jaffé PR. Precipitation of copper (II) in a two-stage continuous treatment system using sulfate reducing bacteria. Waste Biomass Valor 2019;10:2907–14. https://doi.org/10.1007/s12649-018-0329-3.
[51] Costa JM, Rodriguez RP, Sancinetti GP. Removal sulfate and metals Fe^{+2}, Cu^{+2}, and Zn^{+2} from acid mine drainage in an anaerobic sequential batch reactor. J Environ Chem Eng 2017;5:1985–9. https://doi.org/10.1016/j.jece.2017.04.011.
[52] Uçar D. Sequential precipitation of heavy metals using sulfide-laden bioreactor effluent in a pH controlled system. Min Proc Ext Met Rev 2017;38:162–7. https://doi.org/10.1080/08827508.2017.1281131.
[53] Colipai C, Southam G, Oyarzún P, González D, Díaz V, Contreras B, et al. Synthesis of copper sulfide nanoparticles using biogenic H_2S produced by a low-pH sulfidogenic bioreactor. Minerals 2018;8:35. https://doi.org/10.3390/min8020035.
[54] MacPhail PK, Fleming CA, Sarbutt K. Cyanide recovery by the SART process for the lobo-marte project, Chile. In: Randol gold and silver forum; 1998. p. 26–9 [Denver, USA].
[55] Hedjazi F, Monhemius AJ. Copper-gold ore processing with ion exchange and SART technology. Miner Eng 2014;64:120–5. https://doi.org/10.1016/j.mineng.2014.05.025.
[56] Estay H, Gim-Krumm M, Seriche G, Quilaqueo M, Barros L, Ruby-Figueroa R, et al. Optimizing the SART process: a critical assessment of its design criteria. Miner Eng 2020;146:106116. https://doi.org/10.1016/j.mineng.2019.106116.
[57] Baker B, Rodriguez F, Littlejohn P. SART implementation at gold mines in Latin America. In: World gold 2017. CIM/ICM; 2017. p. 27–30. Vancouver, Canada.
[58] Kratochvil D, Salari D, Avilez T. SART implementation at heap leach operations in Mexico. In: 50th Canadian minerals processors conference; 2018. Ottawa, Canada.
[59] Sceresini B, Breuer P. Gold-copper ores. In: Adams MD, editor. Gold ore processing. 2nd ed. Amsterdam: Elsevier; 2016. p. 771–801. https://doi.org/10.1016/B978-0-444-63658-4.00043-8.
[60] Potter GM, Bergmann A, Haidlen U. Process of recovering copper and of optionally recovering silver and gold by leaching of oxide and sulfide-containing materials with water-soluble cyanides. In: U.S. Pat. 1986;4:587. 110.
[61] Mokone TP, van Hille RP, Lewis AE. Effect of solution chemistry on particle characteristics during metal sulfide precipitation. J Colloid Interface Sci 2010;351:10–8. https://doi.org/10.1016/j.jcis.2010.06.027.
[62] Mokone TP, van Hille RP, Lewis AE. Metal sulphides from wastewater: assessing the impact of supersaturation control strategies. Water Res 2012;46:2088–100. https://doi.org/10.1016/j.watres.2012.01.027.
[63] Mokone TP, Lewis AE, van Hille RP. Effect of post-precipitate conditions on surface properties of colloidal metal sulphide precipitates. Hydrometallurgy 2012;119–120:55–66. https://doi.org/10.1016/j.hydromet.2012.02.015.
[64] Nduna M, Rodriguez-Pascual M, Lewis AE. Effect of dissolved precipitating ions on the settling characteristics of copper sulphide. J South Afr Inst Min Metall 2013;113:435–9. http://www.scielo.org.za/scielo.php?script=sci_arttext&pid=S2225-62532013000500009&lng=en&nrm=iso.
[65] Fleming CA, Melashvili M. The SART process: killing the sacred cows. In: XXVIII international mineral processing congress (IMPC 2016); 2016. p. 11–5. Quebec, Canada.
[66] Chen Q, Yao Y, Li X, Lu J, Zhou J, Huang Z. Comparison of heavy metal removals from aqueous solutions by chemical precipitation and characteristics of precipitates. J Water Process Eng 2018;26:289–300. https://doi.org/10.1016/j.jwpe.2018.11.003.
[67] Gim-Krumm M, Quilaqueo M, Rojas V, Seriche G, Ruby-Figueroa R, Cortés-Arriagada D, et al. Impact of precipitate characteristics and precipitation conditions on the settling performance of a sulfide precipitation process: an exhaustive characterization of the aggregation behavior. Hydrometallurgy 2019;189:105150. https://doi.org/10.1016/j.hydromet.2019.105150.
[68] Wrighton-Araneda K, Ruby-Figueroa R, Estay H, Cortés-Arriagada D. Interaction of H_2O with $(CuS)_n$, $(Cu_2S)_n$, and $(ZnS)_n$ small clusters (n=1-4, 6): relation to the aggregation characteristics of metal sulfides at aqueous solutions. J Mol Model 2019;25:291. https://doi.org/10.1007/s00894-019-4161-x.
[69] Deng Z, Oraby EA, Eksteen JJ. Sulfide precipitation of copper from alkaline glycine-cyanide solutions: precipitate characterization. Miner Eng 2020;145:106102. https://doi.org/10.1016/j.mineng.2019.106102.
[70] Quilaqueo M, Gim-Krumm M, Ruby-Figueroa R, Troncoso E, Estay H. Determination of size distribution of precipitation aggregates using non-invasive microscopy and semiautomated image processing and analysis. Minerals 2019;9:724. https://doi.org/10.3390/min9120724.
[71] Yan X, Chai L, Li Q, Ye L, Yang B, Wang Q. Abiological granular sludge formation benefit for heavy metal wastewater treatment using sulfide precipitation. Clean 2017;45:1500730. https://doi.org/10.1002/clen.201500730.
[72] Peng X, Xia Z, Kong L, Hu X, Wang X. UV light irradiation improves the aggregation and settling performance of metal sulfide particles in strongly acidic wastewater. Water Res 2019;163:114860. https://doi.org/10.1016/j.watres.2019.114860.
[73] Breuer P. Dealing with copper in gold ores; implemented and future approaches. In: Proceedings of gold-PM conference, 20th anniversary event. Perth, Australia: ALTA; 2015. p. 23–30.
[74] Estay H, Carvajal P, Hedjazi F, Van Zeller T. The SART process experience in the Gedabek plant. In: HydroProcess 2012, 4th international workshop on process hydrometallurgy; 2012. p. 11–3 [Santiago, Chile].
[75] Simons A, Breuer P. The impact of residence time on copper recovery in Telfer Gold Mine's cyanide recycling process.

World gold 2013. Brisbane, Queensland, Australia: Australasian Institute of Mining and Metallurgy; 2013. p. 189–96. 26-29; Melbourne, Australia.
[76] Simons A. Fundamental study of copper and cyanide recovery from gold tailing by sulfidisation. PhD. Thesis. Perth, WA: WA School of Mines, Curtin University; 2015.
[77] Estay H, Becker J, Carvajal P, Arriagada F. Predicting HCN gas generation in the SART process. Hydrometallurgy 2012;113–114:131–42. https://doi.org/10.1016/j.hydromet.2011.12.019.
[78] Echavarría AP, Torras C, Pagán J, Ibarz A. Fruit juice processing and membrane technology application. Food Eng Rev 2011;3:136–58. https://doi.org/10.1007/s12393-011-9042-8.
[79] Li J, Chase HA. Applications of membrane techniques for purification of natural products. Biotechnol Lett 2010;32:601–8. https://doi.org/10.1007/s10529-009-0199-7.
[80] Cassano A, Ruby-Figueroa R, Drioli E. Membrane separation. In: Food eng. Fundam. Volume I handb. Food Process. Eng.; 2014. p. 1–29.
[81] Saad MA. Early discovery of RO membrane fouling and real-time monitoring of plant performance for optimizing cost of water. Desalination 2004;165:183–91. https://doi.org/10.1016/j.desal.2004.06.021.
[82] Yu CH, Fang LC, Lateef SK, Wu CH, Lin CF. Enzymatic treatment for controlling irreversible membrane fouling in cross-flow humic acid-fed ultrafiltration. J Hazard Mater 2010;177:1153–8. https://doi.org/10.1016/j.jhazmat.2010.01.022.
[83] Marsden JO, House CI. The chemistry of gold extraction. 2nd ed. Englewood, CO, USA: Society for Mining, Metallurgy and Exploration SME; 2006.
[84] Field RW, Wu D, Howell JA, Gupta BB. Critical flux concept for microfiltration fouling. J Memb Sci 1995;100:259–72. https://doi.org/10.1016/0376-7388(94)00265-Z.
[85] Astudillo-Castro CL. Limiting flux and critical transmembrane pressure determination using an exponential model: the effect of concentration factor, temperature, and cross-flow velocity during casein micelle concentration by microfiltration. Ind Eng Chem Res 2015;54:414–25. https://doi.org/10.1021/ie5033292.
[86] Ferreira SLC, Bruns RE, Ferreira HS, Matos GD, David JM, Brandão GC, et al. Box-Behnken design: an alternative for the optimization of analytical methods. Anal Chim Acta 2007;597:179–86. https://doi.org/10.1016/j.aca.2007.07.011.
[87] Van der Bruggen B. Microfiltration, ultrafiltration, nanofiltration, reverse osmosis, and forward osmosis. In: Luis P, editor. Fundamental modelling of membrane systems: membrane and process performance. Amsterdam: Elsevier; 2018. https://doi.org/10.1016/B978-0-12-813483-2.00002-2 [Chapter 2].
[88] Arnot TC, Field RW, Koltuniewicz AB. Cross-flow and dead-end microfiltration of oily-water emulsions. Part II. Mechanisms and modelling of flux decline. J Memb Sci 2000;169:1–15. https://doi.org/10.1016/S0376-7388(99)00321-X.
[89] Hurt EE, Adams MC, Barbano DM. Microfiltration: effect of retentate protein concentration on limiting flux and serum protein removal with 4-mm-channel ceramic microfiltration membranes. J Dairy Sci 2015;98:2234–44. https://doi.org/10.3168/jds.2014-9032.
[90] Barros L, Gim-Krumm G, Seriche G, Quilaqueo M, Castillo C, Ihle CF, et al. Powder Technol 2021;380:205–2018. https://doi.org/10.1016/j.powtec.2020.11.038.